Journal of
Polymer Materials

Tech Science Press

Doi:10.32604/jpm.2025.062481

ARTICLE

Shape Memory Properties of Short-Glass Fiber Reinforced Epoxy Composite Programmed below Glass Transition Temperature

Kartikey Shahi, Velmurugan Ramachandran*, Ranjith Mohan and Boomurugan Ramachandran

Department of Aerospace Engineering, Indian Institute of Technology Madras, Chennai, 600036, India

*Corresponding Author: Velmurugan Ramachandran. Email: ramanv@iitm.ac.in

Received: 19 December 2024; Accepted: 21 March 2025; Published: 11 July 2025

ABSTRACT: A Shape Memory Polymer Composite (SMPC) is developed by reinforcing an epoxy-based polymer with randomly oriented short glass fibers. Diverging from previous research, which primarily focused on the hot programming of short glass fiber-based SMPCs, this work explores the potential for programming below the glass transition temperature (Tg) for epoxy-based SMPCs. To mitigate the inherent brittleness of the SMPC during deformation, a linear polymer is incorporated, and a temperature between room temperature and Tg is chosen as the deformation temperature to study the shape memory properties. The findings demonstrate an enhancement in shape fixity and recovery stress, alongside a reduction in shape recovery, with the incorporation of short glass fibers. In addition to tensile properties, thermal properties such as thermal conductivity, specific heat capacity, and glass transition temperature are investigated for their dependence on fiber content. Microscopic properties, such as fiber-matrix adhesion and the dispersion of glass fibers, are examined through Scanning Electron Microscope imaging. The fiber length distribution and mean fiber lengths are also measured for different fiber fractions.

KEYWORDS: Shape memory polymer composite; glass fiber composite; shape fixity; shape recovery; thermomechanical cycle

1 Introduction

Shape memory polymers (SMPs) are polymers that can retain and regain deformations with different stimuli such as heat, light, electricity, a magnetic field, moisture, and chemicals [1–4]. Compared to Shape Memory Alloys, the SMPs have gained popularity due to their ability to tailor material properties, low cost, ease of manufacturing, and withstand large deformations [5]. Efforts have been made to improve the mechanical and shape memory properties of the polymers with various types of reinforcements like nanoparticles and fibers [6–8]. Shape Memory Polymer Composites (SMPCs) with unidirectional, woven, laminates, and hybrid composites have proven to be a great success in improving the strength and stiffness of SMPCs [9,10]. SMPCs reinforced with knit fabric recently developed exhibited shape fixation ratios above 98% and high recovery efficiency at 100°C actuation temperatures. The anisotropic nature of knitted fabric reinforcement influenced recovery time and mechanical response, with samples in different orientations showing varied performance [11]. However, these fiber architectures do not provide isotropic properties, and certain regions may have a high polymer content, while others have high fiber content. Furthermore, such laminates often struggle to endure large tension or compression strains, limiting their applicability in demanding structural environments. These limitations can be overcome by using randomly dispersed fibers, which provide a more uniform reinforcement and isotropic mechanical properties.

The applications of SMPC include actuators, biomedical devices, aerospace, aviation, and 4D printing & origami [12–14]. A typical application of SMPCs that require large deformation in tension is a variable stiffness morphing wing, where long continuous fibers are unsuitable due to brittle failure, making short elastic fibers the preferred choice by default [15]. The skin of variable camber wing requires the composite material to undergo large stretches. Additionally, SMPCs in tension mode can be utilized to generate high recovery stress or serve as an effective fixation medium [16]. The present study aims to develop SMPCs tailored for these engineering applications.

Short glass and carbon fibers are among the most widely used reinforcements for SMPCs. Short glass fibers, in particular, are preferred due to their excellent fatigue resistance, electrical insulation, corrosion resistance, low cost, and ease of processing and handling [17]. Several studies have explored the effects of short glass fibers on the mechanical properties of SMPCs, showing that fiber reinforcement significantly improves tensile strength and modulus [18,19]. The shape memory properties of short glass fiber-reinforced SMPs have been primarily investigated through hot programming, where the material is heated above its glass transition temperature (Tg) and then cooled to fix a temporary shape [20–23].

A critical factor in achieving optimal shape memory performance is the selection of an appropriate programming temperature [24,25]. While conventional hot programming methods rely on heating the SMPC above its glass transition temperature (Tg), intermediate programming techniques where deformation occurs near Tg followed by cooling have shown promise in balancing shape fixity and recovery. Programming SMPCs below Tg is particularly important for expanding their applicability by enabling large deformations while enhancing energy efficiency. This approach eliminates the need for extensive thermal cycling, thereby reducing processing costs [25]. However, the high strain levels in the cold-drawing process can lead to irreversible damage, which may impact the precision of deformation over repeated cycles [26].

Cold programming, which involves deforming an SMPC at room temperature, has traditionally been considered impractical due to the brittle nature of most SMPCs at lower temperatures [25,27–29]. To mitigate the aforementioned issues, recent advancements in thermoset polymer formulations, such as the incorporation of Neopentyl Glycol Diglycidyl Ether (NGDE) with Epoxy Diglycidyl Ether Bisphenol A (DGEBA), have significantly improved failure strain and damage at temperatures near Tg, making cold programming a viable alternative [30]. This advancement has opened new possibilities for unconventional programming techniques that allow large deformations without the need for extensive heating.

The present study adopts this approach to achieve large deformations (≥0.2) while ensuring effective shape retention and recovery. The mass fraction of short fibers is varied from 0% to 15% to determine the maximum limit at which such deformations can be sustained. This research investigates the mechanical, thermal, and shape memory properties of short glass fiber-reinforced epoxy-based SMPCs at temperatures below Tg to enable large deformations in tension. Key shape memory parameters, including shape fixity, recovery strain, and recovery forces, are analyzed to assess the feasibility of cold programming in these materials. Additionally, Scanning Electron Microscopy is utilized to examine fractured surfaces and fiber length distribution, while thermal properties such as thermal conductivity and glass transition temperature are also characterized. By exploring how fiber reinforcement influences the trade-offs between shape fixity and recovery, this study provides valuable insights into optimizing SMPCs for real-world applications requiring large deformations and precise shape memory behavior. Future research should further investigate the impact of different fiber types, orientations, and programming conditions to enhance the overall performance and applicability of SMPCs.

2 Experimental Details

2.1 Material

This study uses Diglycidyl Ether Bisphenol A (DGEBA) and Neopentyl Glycol Diglycidyl Ether (NGDE) as the polymeric materials investigated. Poly(propylene glycol) bis(2-aminopropyl) ether (Jeffamine230) is used as a crosslinker to form a thermoset polymer. For reinforcement, finely chopped glass fibers SE 1043, pre-treated with proprietary sizing, are sourced from 3B-Fiber Glass. It has a filament diameter of 24 μm, a mean fiber length of 3.36 mm, and a density of 2.55 g/cc. The polymers are obtained from Sigma Aldrich. The properties of the materials used are given in Table 1.

Table 1: Polymer properties

Material	Molecular weight (g/mol)	Viscosity (MPa·s)	Density (g/cc)
DGEBA	340.4	11,000.0	1.22
NGDE	216.2	20.0	1.08
Jeffamine 230	230.0	5.5	0.95

2.2 Fabrication of SMPC

The most common techniques to fabricate these laminates are extrusion compounding and injection molding. However, due to the smaller fiber mass fraction (≤15%) and to ensure random orientation, we follow a procedure of stirring and moulding to fabricate laminates. First, silicone rubber molds are blanked out for the Dog bone shape as per American Society for Testing and Materials (ASTM) D638 IV using MAXIEM water jet cutting to create samples for tensile and shape memory tests. Additionally, rectangular blank outs of 10 mm × 6 mm and circular blank outs of 12.5 mm diameter × 4 mm height are also cut to prepare samples for the DMA and the Laser/Light Flash Analyzer (LFA), respectively. Mylar sheets and glasses are cut into rectangular shapes to hold the rubber mold from both sides using clamps.

Once the setup is ready, the polymers are mixed in the desired ratio. To obtain better material properties of SMPC, the ratio of DGEBA to NGDE considered here is 75 to 25, as discussed in Section 3. Jeffamine 230 is used as a cross-linker or hardener. The weight of Jeffamin 230 is determined according to the method mentioned in [29]. The short glass fibers are heated with acetone to remove any moisture or chemicals present on them until they dry out properly. They are immediately added to the resulting polymer mixture and mixed thoroughly with a magnetic stirrer. Different fiber mass fractions are added: 0%, 5%, 7.5%, 10%, and 15%. Usually, bubbles are formed during magnetic stirring, which need to be removed. To address this, the resulting mixture is placed into a vacuum chamber for 5 min to eliminate trapped air. The mixture is then taken out and poured into the mold, which should be properly coated with wax for easy removal of samples after curing. The level of the entire mold setup is adjusted using a level meter. It is allowed to cure at room temperature for 24 h.

Finally, the mold is placed inside the oven, and the sample is post-cured at 80°C for 2 h. The samples are separated from the mold and used for testing purposes 24 h later.

2.3 Measurements

2.3.1 Tensile Testing

The tensile specimens are tested using a temperature-controlled Kalpak 20N Universal Testing Machine (UTM). The samples are tested at 30°C, 40°C, and 75°C, respectively. First, the samples are placed inside

the chamber and heated to the set point, allowed to attain thermal equilibrium for 30 min. This ensures temperature uniformity throughout the sample. Finally, the samples are stretched with a cross-head speed of 2 mm/min until failure.

2.3.2 Thermal and Glass Transition Properties

The properties, such as thermal conductivity and specific heat capacity, are measured using the NETZSCH LFA 467 HyperFlash Thermal Analyzer. The samples, with a diameter of 12.5 mm and a height of 4 mm, are first coated with graphite to enhance the absorption and emission properties of the sample. This coating allows for more accurate measurements. The reference sample considered is Pyroceram, used to measure the thermal properties. Three shots are taken in each laser flash at 0°C, 20°C, 40°C, 60°C, and 80°C, to determine these properties.

The Dynamic Mechanical Analyzer (DMA), NETZSCH DMA 242 E, is utilized to study the glass transition behavior of SMPC. DMA is a tool mainly used to measure the viscoelastic properties of polymers and composites in dynamic and static conditions. In the present work, the temperature is increased from 0°C to 100°C at a rate of 4°C/min, and a dynamic load of 5 N is applied with a frequency of 1 Hz in the dynamic module of DMA. Tan δ is measured, representing the ratio of the loss modulus to the storage modulus. Although there are various definitions and measurement methods for glass transition, in this study, the peak of Tan δ is considered as the glass transition temperature of the material.

The DMA includes a creep module capable of measuring the strain of a sample subjected to a load. Additionally, it can be used to measure the strain of stress-free thermal expansion. The creep load is set to 0.001 N, and the temperature is ramped from 0°C to 100°C with a rate of 4°C/min in this study. The tangent to the curves on the strain-temperature plot provides the Coefficient of Linear Thermal Expansion (CLTE). CLTE is measured for both the glassy and rubbery phases. Various fixtures are available to hold the specimen, including three-point bending, compression, and tension. In this case, the tension-type fixture holds the samples with dimensions of 10 mm × 6 mm × 2 mm.

2.3.3 Shape Memory Properties

Two important shape memory properties are shape fixity and shape recovery. The SMPC is subjected to tensile deformation at the desired temperature. During the cooling step, a new shape is formed, which is retained after the unloading step. Shape fixity measures the ratio of fixed strain to maximum deformation strain after the unloading step.

$$S_f = \frac{\varepsilon_f}{\varepsilon_p} \tag{1}$$

where S_f is shape fixity, ε_f is fixed strain, and ε_p is programming strain. To obtain the original shape, the SMPC is reheated to a temperature above T_g. Shape recovery measures the ratio of recovered strain to the fixed strain.

$$R_r = \frac{\varepsilon_f - \varepsilon_r}{\varepsilon_f} \tag{2}$$

where R_r is the recovery ratio, ε_f is the fixed strain, and ε_r is a non-recoverable or residual strain. In the current study, strain is measured using the Digital Image Correlation (DIC) technique. The samples are coated with white paint, and black dots are sprayed on the top for visibility. The VIC 2D software is employed for image processing and correlation.

Initially, the sample is loaded into the UTM at 40°C and allowed to reach thermal equilibrium for 30 min. The camera, mounted on a tripod, is activated to capture images of the sample visible through the chamber's glasses at a rate of 15 frames per minute. Loading continues until the sample is strained to 20% of its original length, followed by stress relaxation for 45 min while slowly cooling it to 30°C. To unload the sample, the chamber is opened, and the grips are released. The frame rate is set at 15 frames per minute during the loading and recovery stages, while it is adjusted to 1 frame per second for the unloading phase to capture spring back. Subsequently, the chamber is closed, and the sample is reheated to 80°C at a rate of 4°C per minute. Two recovery scenarios are considered: free recovery and constrained recovery. In free recovery, the sample is not gripped, while in constrained recovery, the sample is gripped, and stress values are recorded in the UTM. This experiment is repeated with different samples having varying fiber mass fractions.

2.3.4 Microscopy

Scanning Electron Microscopy is conducted using Inspect F50, a high-resolution Scanning Electron Microscope based on a field emission gun. Samples for SEM are obtained by cutting fractured tensile specimens to ensure that the fractured surfaces are visible under the SEM. Gold coating is applied to the exposed surface of the sample. Subsequently, the sample is positioned in the SEM, and images are captured at various locations and resolutions, ranging from 300x to 2000x. The length distribution of glass fibers embedded in the polymer matrix is also measured to better understand their reinforcing effect. This process begins with a burnout test, where the composite sample is heated to 600°C for 24 h. During this high-temperature treatment, the polymer matrix is completely burned away, leaving only the glass fibers intact. These residual fibers are then carefully collected and transferred to a glass slide. To facilitate their dispersion, small droplets of water are added to the slide, allowing the fibers to spread out uniformly. Once the fibers are well-dispersed, the slide is placed under a Dino Lite microscope equipped with length measurement capabilities. The magnification factor is varied between 30x to 45x. High-resolution images are captured, and the lengths of a representative sample of fibers are measured using the microscope's software, DinoCapture 2.0. This method ensures a precise and accurate determination of the fiber length distribution within the composite.

3 Results and Conclusion

The flexible linear polymer NGDE not only lowers the Tg but also increases the failure strain [29]. However, the polymer has less viscosity which decreases the overall viscosity of DGEDBA and NDGE polymer mixture, Table 1. This causes high-density glass fibers to settle down inside the mold due to gravity in a freshly prepared resin and fiber mixture. The hit and trial in experiments suggest that the suitable amount of DGEBA:NGDE to be used is 75:25 for fibres to suspend and result in uniform dispersion.

3.1 Mechanical Properties

The epoxy-based short glass fiber-reinforced Shape Memory Polymer Composite (SMPC) exhibits a dependence on mechanical properties concerning temperature and fiber content. Understanding properties such as yield strength and failure strain of SMPC is crucial for large-deformation applications. The selection of programming variables, such as deformation temperature and strain, is based on the aforementioned mechanical properties.

The stress-strain curve for the SMPC at 30°C with varying fiber content is depicted in Fig. 1. The fiber mass fraction of randomly oriented short glass fibers ranges from 0% to 15%. The neat polymer has an elastic modulus of 310.5 MPa and a yield stress of 25.4 MPa at a temperature of 30°C. As observed, it exhibits viscoelastic-plastic behavior at this temperature. It behaves elastically until the nominal strain value

of 0.1, followed by strain-softening and a steady zone. Deformations beyond the yield limit consist of both recoverable and irrecoverable components of strain.

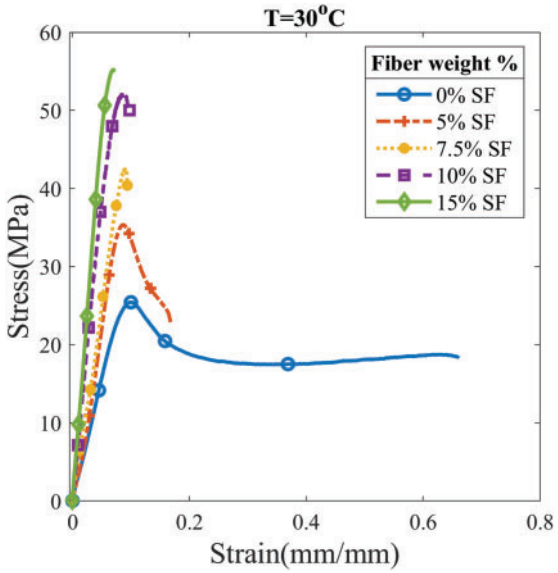

Figure 1: Stress response of SMPC at 30°C with increasing mass fraction of short glass fibers

The failure of SMPC occurs at a nominal strain value of 0.66 or a strain percentage of 66.0%. This behavior of neat SMP can be attributed to the presence of polymer chains that initially resist deformation. Subsequently, intermolecular segments begin rotating after reaching the yield stress until the cross-linked chains resist further deformation, leading to strain-hardening before failure [18].

Further, the addition of short glass fibers changes the mechanical properties of SMPC. As seen in the Fig. 1, the tensile modulus, yield strength, and failure strain vary with different fiber mass fractions. The tensile modulus increases from 0.31 to 0.96 GPa and yield strength from 25.39 to 55.20 MPa for the neat polymer to 15% mass fraction of short glass fibers, respectively, at 30°C. The composite strength here is the maximum stress that can be resisted by SMPC, which is equal to yield strength in this particular case, see Fig. 1. The increase in aforementioned properties can be attributed to the presence of glass fibers that act as stiff reinforcement and participate in load sharing. The three most important parameters affecting the properties of SMPC are fiber volume, fiber length, and orientation. In the present work, the fiber mass fraction can be considered as the major contributing factor to the change in the properties. However, as the mass fraction of fibers is increased from 0% to 15%, the failure strain decreases from 0.66 to 0.09. This can be attributed to stress concentration at the endpoint of fibers, which causes matrix crack formation and propagation until the failure [31,32]. As seen in Fig. 1, the SMPC without any fibers exhibits a zone of steady plastic flow post-yielding. Due to short fibers, the SMPC becomes brittle and cannot sustain large plastic deformations. Recent surface treatment methods, such as acid treatment of fibers, have been shown to have significant improvements in elongation at break and tensile modulus [33]. Implementing such techniques in future work could help further mitigate the brittleness of fibers observed in the present study, potentially enhancing both the mechanical performance and durability of the composite.

The SMP is considered to have crosslinks that behave as hyperelastic and entangled polymer chains that act in a viscoelastic-plastic manner [34]. Both segments participate in load sharing on deformation. The viscoelastic-plastic behaviour of the polymer depends on viscosity, which in turn greatly depends on

temperature. The addition of randomly oriented short fibers results in a homogeneous and isotropic SMPC and thus exhibits similar behaviour as SMP.

The stress response of SMPC at 40°C is depicted in Fig. 2. The tensile modulus increases from 0.19 to 0.50 GPa and yield strength from 10.28 to 31.36 MPa for the neat polymer to 15% mass fraction of short glass fibers, respectively, at 40°C. The SMPC becomes more rubbery due to the decreased viscosity of polymer with an increase in temperature, however, this temperature is still below the T_g of SMPCs which is around 60°C, discussed in the next section. The segments rotate easily and offer less resistance to plastic deformation. As temperature increases from 30°C to 40°C, the failure strain increases from 0.66 to 1.13, 0.17 to 0.65, 0.09 to 0.50, 0.07 to 0.14 for fiber mass fraction of 0%, 5%, 7.5%, 10%, 15%. It is therefore evident that crack formation and propagation are reduced at this temperature resulting in high failure strain. Comparing SMPC behaviour at two different temperatures, we can see that tensile modulus and yield strength drop and failure strain increase at 40°C as compared to 30°C. The increase in failure strain makes it suitable for large deformations at 40°C.

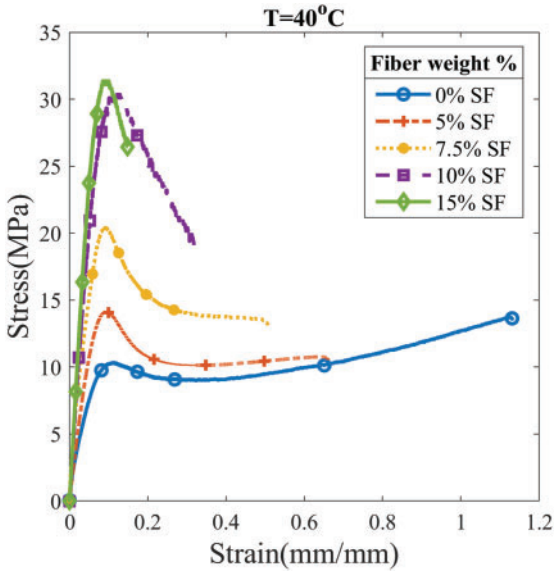

Figure 2: Stress response of SMPC at 40°C with increasing mass fraction of short glass fibers

If the temperature is increased above T_g up to a point where the viscosity of polymer chains flowing past each other becomes zero, only the cross-link participates in load sharing. This results in pure hyperelastic behaviour. Fig. 3 shows the stress response of SMPC at 75°C. At this temperature, the material becomes very soft and behaves as hyperelastic material. The tensile modulus of SMPC at 75°C are 6.81, 12.42, 20.54, 42.72, and 44.74 MPa and failure strain of 0.49, 0.21, 0.15, 0.12, and 0.10 for SMPC with fiber mass fraction of 0%, 5%, 7.5%, 10%, 15%.

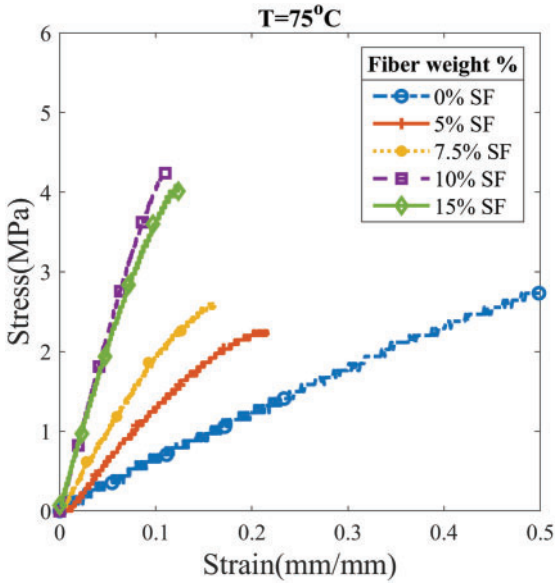

Figure 3: Stress response of SMPC at 75°C with increasing mass fraction of short glass fibers

3.2 Microscopic Properties

3.2.1 Scanning Electron Microscopy

The effect of fiber-matrix adhesion and failure mechanism can be inspected through microscopic images obtained from Scanning Electron Microscopy (SEM). The quality of the fibre-matrix interface greatly influences the composite's strength and effective modulus. The failure strain of the composite also depends on fiber breakage and pullout, tensile microcracking, shear yielding, and cracking [35]. Fig. 4 presents SEM images that reveal the random dispersion of short fibers embedded in the matrix of a fractured composite sample surface.

The SEM images show that the fibers are randomly oriented in all directions, refer to A in Fig. 4 embedded in the matrix facilitates load sharing, thereby enhancing the composite's modulus. The quality of fiber-matrix adhesion can be understood through region B, which depicts the residual of matrix on the fiber. Strong adhesion ensures effective stress transfer between fibers and the matrix, contributing to increased composite strength. Poor adhesion can result in fiber pull-out (shown as E) and debonding, weakening the composite structure. The pull-out of fibers dissipates energy during fracture, impacting the toughness and ductility of the composite. The SEM images also show occasional fiber clusters within the matrix, see C in Fig. 4. These clusters can create localized regions of stiffness but may also act as stress concentrators, potentially initiating cracks under load and leading to premature failure. Further, the breakage points, shown as region D, act as sites for stress concentration, which can propagate cracks through the matrix, contributing to the composite's failure.

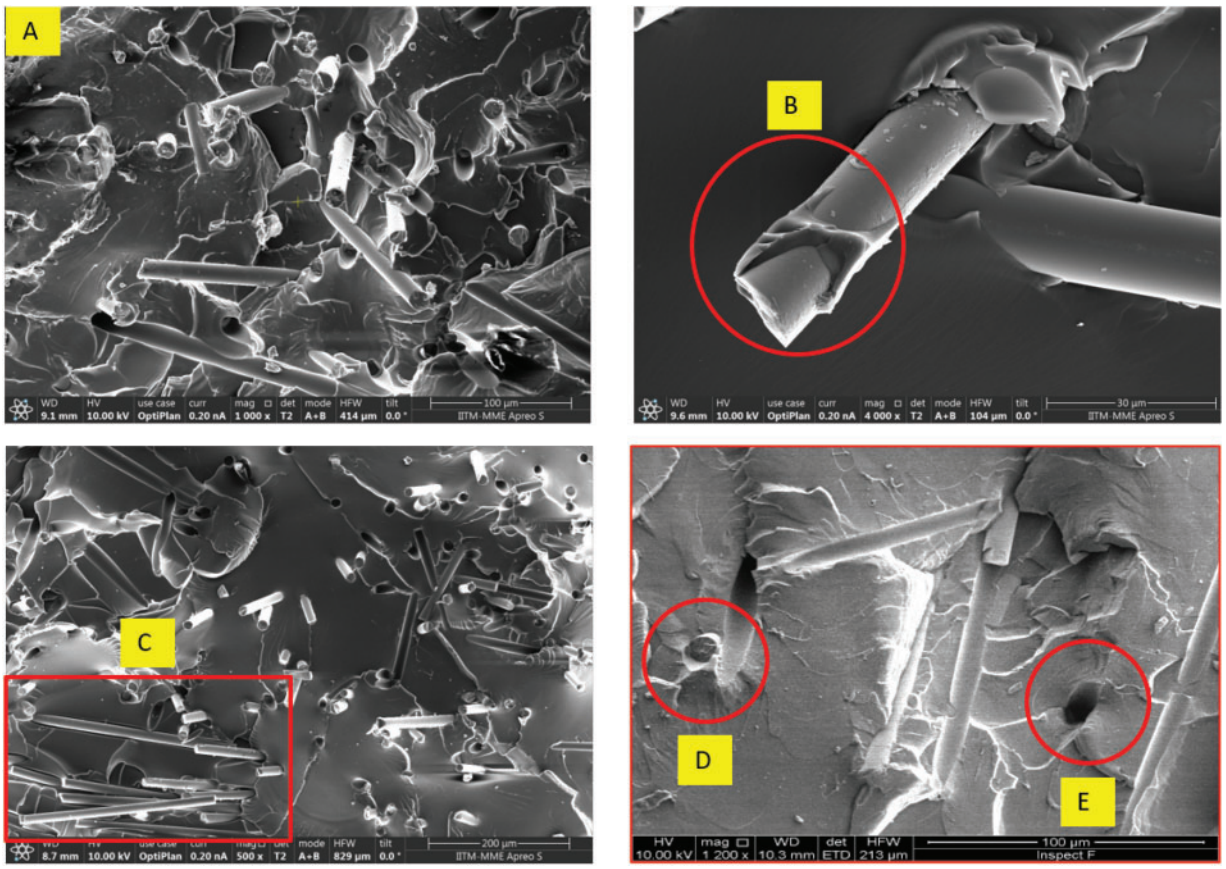

Figure 4: Scanning Electron Microscopy images of the fractured surface of tensile sample with A-random orientation, B-fiber matrix adhesion, C-occasional fiber clusters, D-fiber breakage, and E-fiber pull out

3.2.2 Fiber Length Distribution

The fiber length distribution of glass fibers plays a crucial role in determining the mechanical and thermal properties of the composite. During the shear mixing process, fibers can break down into smaller segments, altering the length distribution. To study this distribution, the lengths of fibers obtained from burnout samples are measured. An in-house developed Python code is used to detect the fibers, measure their lengths, and perform statistical calculations on the data.

Histograms for SMPC with 5%, 7.5%, 10%, and 15% mass fractions of short glass fibers are shown in Figs. 5–8, with the mean length and standard deviation indicated in the graphs. The histograms reveal that a significant number of fibers have lengths close to the mean fiber length, although some very short and very long fibers are also present. This distribution suggests that while the majority of the fibers are broken into manageable lengths during processing, a range of fiber lengths still exists.

The mean fiber length decreases from 0.79 to 0.50 mm as the fiber mass fraction increases from 5% to 15%. This decrease in mean length with increasing fiber content can be explained by the higher probability of fiber breakage during mixing due to the increased interaction between fibers. The presence of shorter fibers at higher mass fractions can adversely affect the load transfer efficiency and the reinforcing effect of the fibers, potentially impacting the overall mechanical properties of the composite. Another crucial factor is whether the fibers are sized or unsized. Literature suggests that fiber sizing enhances interfacial adhesion with the matrix. Additionally, techniques such as coating fibers with polycaprolactone nanoparticles improve

interfacial self-healing capability [36]. In the present work, pre-treated fibers with proprietary sizing were used to ensure effective bonding.

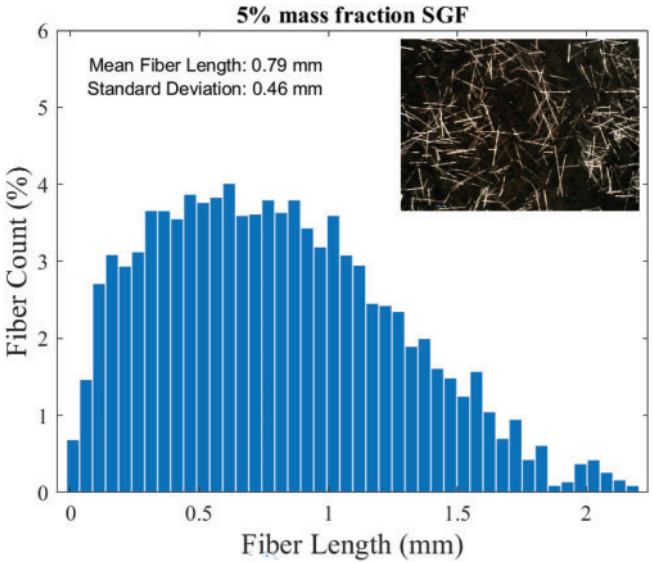

Figure 5: Fiber length distribution of short glass fibers in the samples with 5% mass fraction of fibers

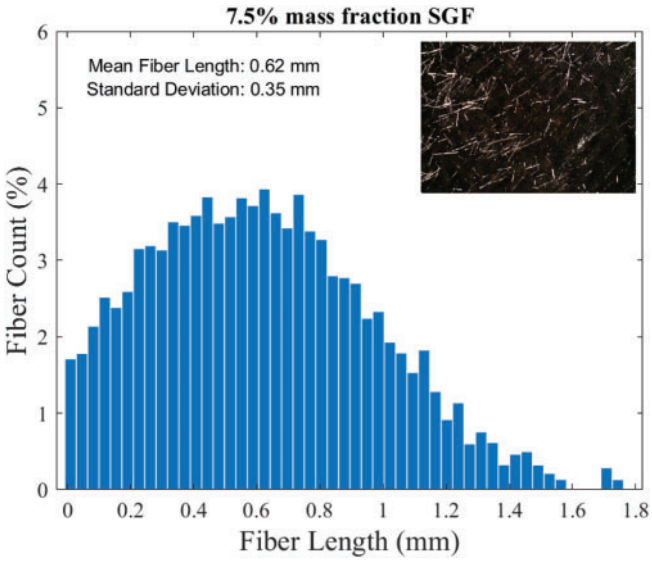

Figure 6: Fiber length distribution of short glass fibers in the samples with 7.5% mass fraction of fibers

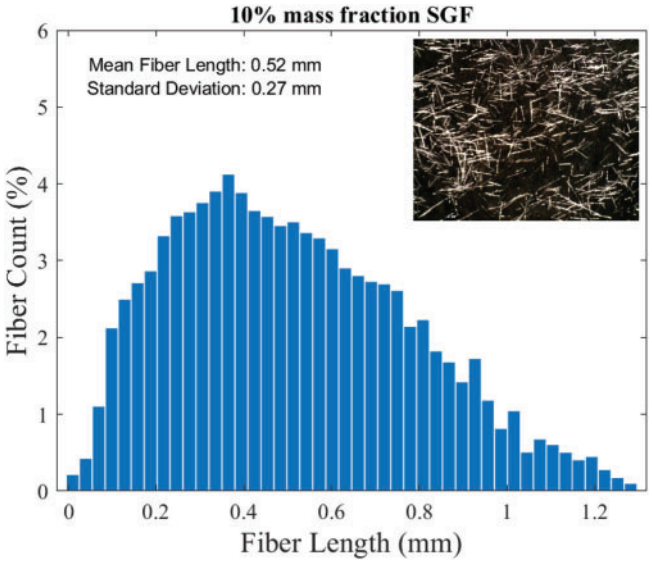

Figure 7: Fiber length distribution of short glass fibers in the samples with 10% mass fraction of fibers

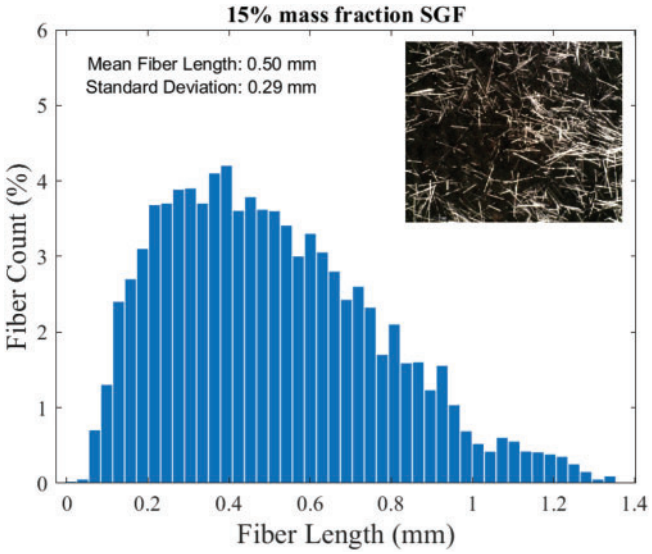

Figure 8: Fiber length distribution of short glass fibers in the samples with 15% mass fraction of fibers

In summary, the fiber length distribution and fiber-matrix adhesion are critical factors that influence the mechanical performance and shape memory properties of glass fiber-reinforced epoxy composites. These aspects must be carefully controlled and optimized to achieve desired performance characteristics in various applications.

3.3 Thermal Properties

The thermal properties of SMPC play a crucial role in determining the programming conditions and also define its application. The most important property of SMPC is the transition temperature around which the shape change is achieved. The glass transition temperature (T_g) is a critical thermal property that indicates

the transition of the polymer from a hard, glassy state to a soft, rubbery state. T_g is measured using a DMA at a frequency of 1 Hz, with a heating rate of 4°C per minute. The peak of the tan delta (tan δ) curve, which represents the ratio of loss modulus to storage modulus, signifies T_g. Fig. 9 illustrates the tan δ curves for SMPCs with different fiber mass fractions. The T_g increases from 61.4°C for neat SMP (0% fiber) to 64.1°C for SMP with 15% fiber mass fraction. This increase in T_g with higher fiber content can be attributed to the restricted molecular mobility of the polymer chains due to the presence of rigid glass fibers, which impede the segmental motion required for the glass transition [37].

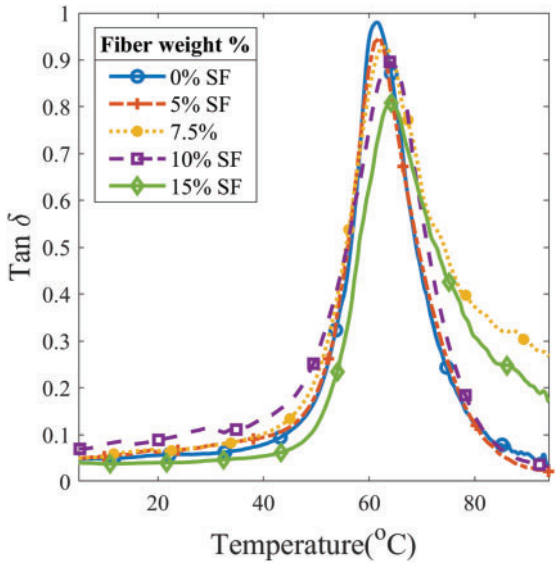

Figure 9: Tan delta (loss modulus/storage modulus) and temperature of SMPC measured by DMA at 1 Hz frequency

The CLTE quantifies the extent to which a material expands upon heating. CLTE is measured from the slope of the strain vs. temperature plot obtained during stress-free thermal expansion using DMA. As shown in Fig. 10, CLTE varies significantly between the glassy and rubbery states of SMPC. In the glassy state (below T_g), CLTE decreases from 0.00039 for neat SMP to 0.00023 for SMP with 15% fiber mass fraction. In the rubbery state (above T_g), CLTE drops from 0.0024 for neat SMP to 0.0005 for the composite with the highest fiber content. The reduction in CLTE with increasing fiber content is due to the lower thermal expansion of glass fibers compared to the polymer matrix. The presence of fibers restricts the thermal expansion of the composite, particularly in the rubbery state where the polymer matrix is more flexible.

Thermal conductivity is an important property for materials used in thermal management applications. It is measured using the NETZSCH LFA 467 HyperFlash Thermal Analyzer. The thermal conductivity of SMPCs increases with higher fiber mass fractions and decreases with increasing temperature. Fig. 11 shows that at 40°C, the thermal conductivity of SMPCs increases from 0.118 W/m·K for neat SMP to 0.164 W/m·K for SMP with 15% fiber mass fraction. At 80°C, the thermal conductivity decreases to 0.094 W/m·K for neat SMP and 0.137 W/m·K for the composite with 15% fiber mass fraction. This trend can be explained by the higher intrinsic thermal conductivity of glass fibers compared to the polymer matrix. The reduction of thermal conductivity with increased temperature of epoxy polymer and increase with increasing filler content has also been reported in the literature [38].

Specific heat capacity (C_p) measures the amount of heat required to raise the temperature of a unit mass of a material by one degree Celsius. C_p is also measured using the NETZSCH LFA 467 HyperFlash Thermal

Analyzer. Fig. 12 indicates that the specific heat capacity of neat SMP increases from 1.36 J/g·K at 0°C to 2.29 J/g·K at 80°C. At 40°C, C_p decreases from 2.24 J/g·K for neat SMP to 1.80 J/g·K for SMP with 15% fiber mass fraction. The decrease in C_p with increasing fiber content can be attributed to the lower specific heat capacity of glass fibers compared to the polymer matrix. The presence of fibers reduces the overall heat capacity of the composite, making it less sensitive to temperature changes.

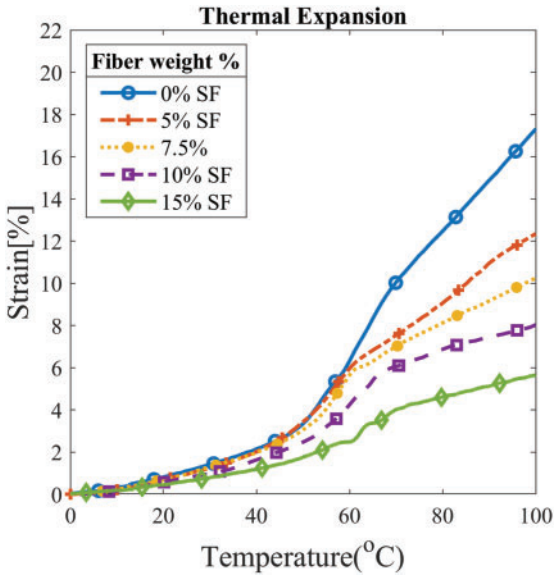

Figure 10: Stress-free thermal expansion of SMPC for different fiber mass fractions measured by DMA in creep mode

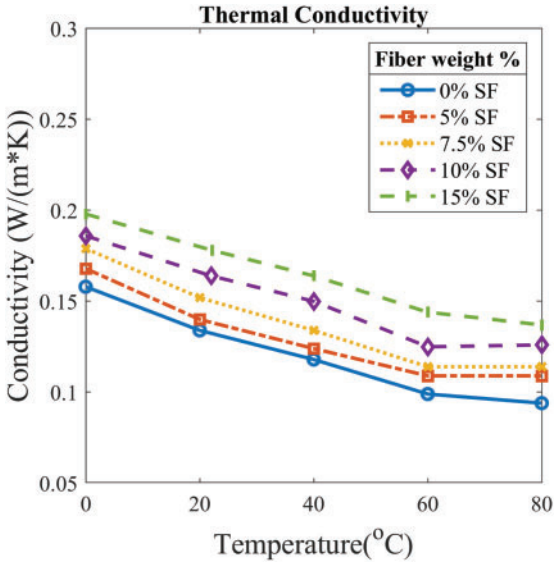

Figure 11: Thermal conductivity of SMPC at different temperatures and fiber mass fractions

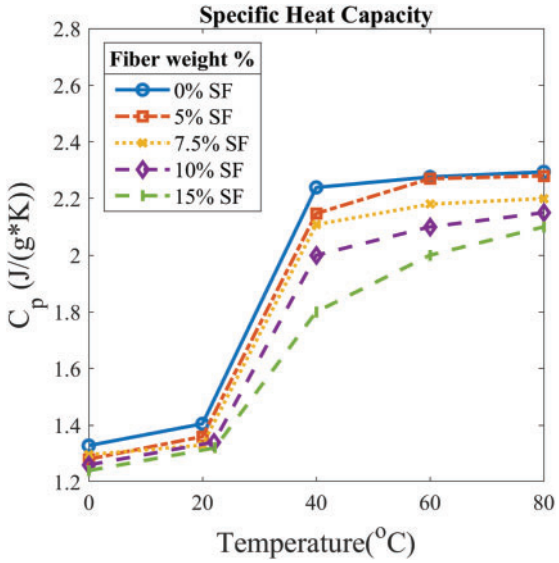

Figure 12: Specific heat capacity of SMPC at different temperatures and fiber mass fractions

The incorporation of short-chopped glass fibers into SMPs significantly influences their thermal properties. The increase in T_g with higher fiber content is due to the restricted molecular mobility of the polymer chains. The decrease in CLTE with increasing fiber content is a result of the lower thermal expansion of glass fibers. Similarly, the enhancement in thermal conductivity with higher fiber content is attributed to the superior thermal conductivity of glass fibers. However, the thermal conductivity decreases with increasing temperature due to increased molecular motion within the polymer matrix. Lastly, the reduction in specific heat capacity with higher fiber content reflects the lower heat capacity of glass fibers compared to the polymer matrix.

3.4 Shape Memory Properties

The study focuses on the shape memory properties of an epoxy polymer composite reinforced with randomly dispersed short chopped glass fibers. The mass fraction of the fibers is varied from 0% to 15%, with significant attention given to the shape memory performance at a deformation temperature of 40°C, which is below the glass transition temperature (Tg) of the composite. This section delves into the experimental findings and the implications of varying fiber content on shape fixity, shape recovery, and recovery stress. The thermomechanical cycles performed in this study involve heating the sample to 40°C, deforming it to the specified strain, holding the deformation while cooling to 30°C, unloading, and finally reheating to 75°C for shape recovery. These cycles are crucial in evaluating the shape memory behavior under different recovery conditions.

The results of the thermomechanical cycles, depicted in Fig. 13 for fiber mass fractions of 0%, 5%, 7.5%, and 10%, show a clear trend of increasing shape fixity with higher fiber content. This indicates that the addition of short chopped glass fibers enhances the ability of the composite to maintain its deformed shape after cooling and unloading.

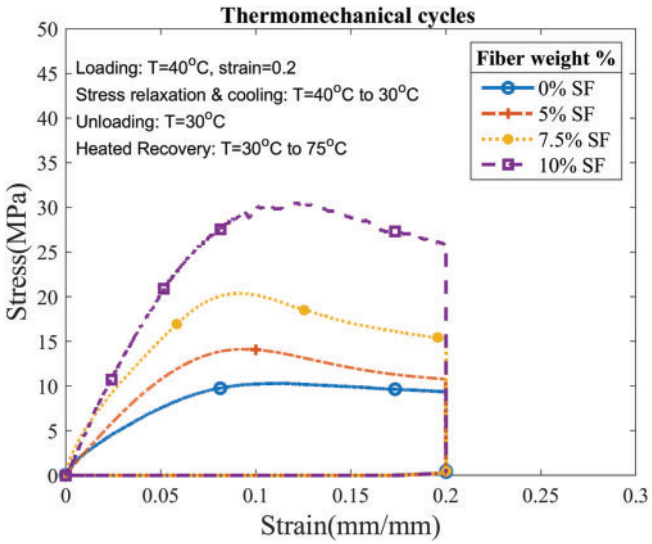

Figure 13: Stress response of short glass fiber reinforced SMPC subjected to a complete thermomechanical cycle for different fiber mass fractions

3.4.1 Influence of Deformation Temperature

The deformation temperature plays a significant role in determining the mechanical performance and shape memory behavior of the composite. In this study, a deformation temperature of 40°C is chosen. This temperature is below the Tg of the polymer matrix but sufficiently high to allow some degree of molecular mobility without surpassing the polymer's glassy state.

Experimental observations reveal that at 40°C, the failure strain is higher than at both 30°C and 75°C. At temperatures below Tg, such as 30°C, the polymer matrix remains relatively rigid, limiting the extent of deformation. Conversely, at temperatures above Tg, such as 75°C, the polymer becomes too soft, and large deformation strains are not achievable due to early material failure. Therefore, 40°C strikes a balance, providing an optimal condition for deformation without compromising the structural integrity of the composite.

3.4.2 Programming Conditions and Strain

The shape memory properties are highly sensitive to the programming conditions, including deformation strain, deformation temperature, holding time, heating rate, and applied loads. In this study, the deformation strain is maintained at 20% for fiber mass fractions up to 10%. This consistent deformation strain allows for a comparative analysis of the influence of fiber content on shape memory performance.

For the composite with a 15% fiber mass fraction, the fracture strain is around 15%, indicating that it is not feasible to achieve a 20% deformation strain without causing material failure. This limitation underscores the need to adjust the programming strain based on the fiber content to avoid premature failure and to ensure effective shape memory performance.

3.4.3 Shape Fixity

Shape fixity is a critical parameter in evaluating the shape memory performance of the polymer composites. It quantifies the ability of the composite to fix the deformed shape upon cooling and unloading. The shape fixity (S_f) is calculated using the Eq. (1). Fig. 14 demonstrates that as the fiber mass fraction increases

from 0% to 10%, the shape fixity of the composites improves from 85.3% to 88.6%. This enhancement in shape fixity with increasing fiber content can be attributed to the reinforcing effect of the glass fibers, which provide additional mechanical stability to the deformed shape. The fibers help in restricting the polymer matrix from relaxing back to its original shape, thereby improving the ability of the composite to retain the deformed configuration.

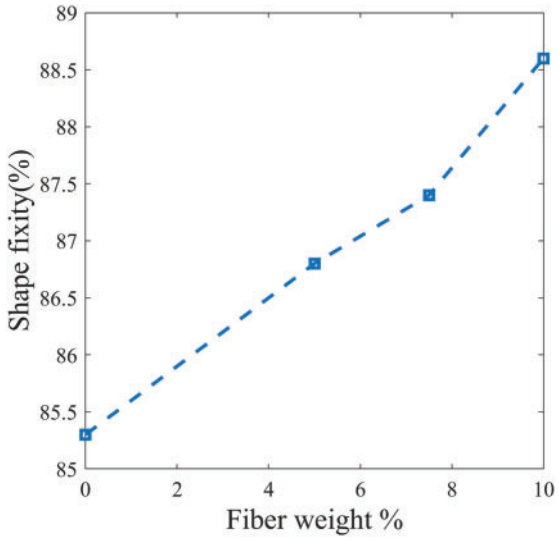

Figure 14: Effect of fiber mass fraction on the shape fixity of short glass fiber reinforced SMPC

3.4.4 Shape Recovery

Shape recovery is another crucial aspect of shape memory behavior, representing the material's ability to return to its original shape upon reheating. In this case, the SMPC is heated from 30°C to 80°C at 4°C/min. The shape recovery ratio (R_r) is given by Eq. (2). The study considers two scenarios for shape recovery: free recovery and fully-constrained recovery. In free recovery, the composite is allowed to recover without any external constraints, whereas, in fully constrained recovery, the composite is restricted from shrinking during the heating process, leading to the generation of recovery stress. The free recovery results, shown in Fig. 15, indicate a significant reduction in shape recovery ratio with increasing fiber content. For a fiber mass fraction of 0%, the shape recovery ratio is 98.63%, which decreases to 90.78% when the fiber content is increased to 10%. This decrease can be explained by the interaction between the polymer matrix and the glass fibers. While the fibers enhance the mechanical properties and shape fixity, they also hinder the polymer chains' mobility during the recovery process. This restriction reduces the material's ability to return fully to its original shape, leading to a lower recovery ratio. The balance between shape fixity and recovery depends on the application. In practical applications such as deployable aerospace structures and medical devices, a high shape fixity ensures that components retain their programmed configurations until activation, while a high shape recovery guarantees the return to their original shapes upon stimulus. The typical range of shape fixity and shape recovery in tension for existing SMPs programmed in warm and cold zones of programming temperature lies between 70%–90% and 90%–100% [25]. Compared to existing fiber-reinforced SMPCs, the proposed material demonstrates an improved fixity-recovery balance due to optimized fiber content, ensuring that stiffness and deformation capabilities are maintained without excessive compromise in recovery.

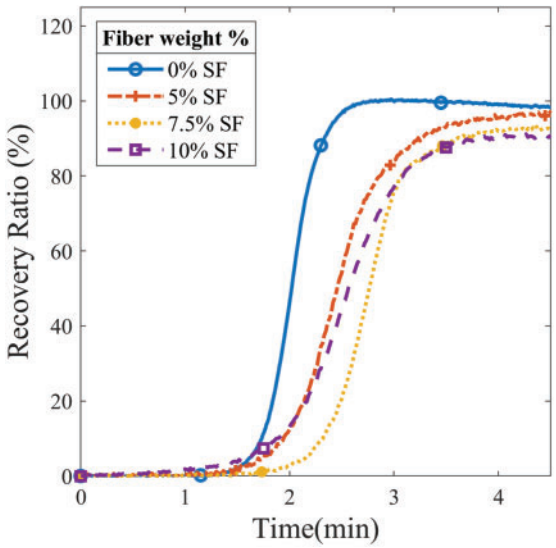

Figure 15: Recovery strain of stress-free SMPC on heating the sample from 30°C to 80°C at 4°C/min

In the fully-constrained recovery scenario, the focus shifts to the recovery stress, which is the stress exerted by the composite as it tries to return to its original shape under constrained conditions. Fig. 16 illustrates that the recovery stress increases from 2.35 to 4.48 MPa as the fiber content rises from 0% to 10%. This increase in recovery stress with higher fiber content is a result of the higher stiffness imparted by the glass fibers. When the composite is heated, the polymer matrix attempts to shrink back, but the fibers resist this movement, thereby generating higher stresses.

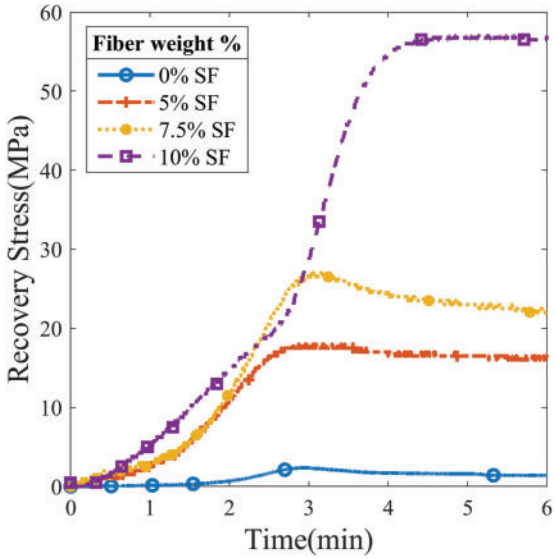

Figure 16: Recovery stress of fully constrained SMPC on heating the sample from 30°C to 80°C at 4°C/min

In contrast, the shape recovery behavior, particularly under free recovery conditions, deteriorates with increasing fiber content. The decrease in recovery ratio suggests that while the fibers improve fixity, they also impede the polymer's ability to fully recover its original shape. This trade-off between shape fixity and shape

recovery must be considered in practical applications, depending on whether the priority is to maintain the deformed shape or to ensure complete recovery. These results highlight the complex interplay between fiber content and shape memory behavior in polymer composites. The findings provide valuable insights for tailoring the composite's properties to meet specific application requirements, whether the focus is on maintaining a deformed shape or ensuring complete recovery. Future work could explore the effects of different fibre types and orientations, as well as the influence of varying programming conditions, to further enhance the understanding and performance of shape memory polymer composites.

4 Summary

In this study, a short glass fiber reinforced Shape Memory Polymer composite based on epoxy is investigated for the mechanical, thermal, microscopic, and shape memory properties. The mechanical properties of SMPCs are significantly influenced by fiber content and temperature. Increasing the short glass fiber content enhances the tensile modulus and yield strength, but reduces the failure strain. At 30°C, the tensile modulus increases from 0.31 to 0.96 GPa, and the yield strength from 25.39 to 55.20 MPa, as the fiber content increases from 0% to 15%. However, higher fiber content makes the SMPC more brittle, reducing its ability to sustain large deformations.

The fiber length distribution is critical for the composite's performance. Higher fiber mass fractions lead to shorter mean fiber lengths due to increased breakage during processing. This decrease in fiber length negatively impacts the load transfer efficiency and mechanical properties.

The thermal properties, including the glass transition temperature (Tg), coefficient of linear thermal expansion (CLTE), thermal conductivity, and specific heat capacity, are all influenced by fiber content. Higher fiber content restricts polymer chain mobility, increasing Tg from 61.4°C for neat SMP to 64.1°C for SMP with 15% fiber. CLTE decreases with higher fiber content, especially in the rubbery state. Thermal conductivity increases with fiber content but decreases with temperature, while specific heat capacity decreases with fiber content.

The shape memory performance is heavily dependent on fiber content and programming conditions. At a deformation temperature of 40°C, which is below Tg, the composite with 10% mass fraction of short glass fibers exhibits shape fixity of 88.6%, recovery ratio of 90.8%, and constraint recovery force of 4.48 MPa (having an ultimate tensile strength of 30.6 MPa). Higher fiber content improves shape fixity but reduces the shape recovery ratio, highlighting a trade-off between maintaining a deformed shape and ensuring complete recovery. The recovery stress increases with fiber content, indicating higher stiffness.

In summary, incorporating short glass fibers into epoxy-based SMPCs enhances their mechanical and thermal properties while introducing a balance between shape fixity and recovery. These insights are valuable for tailoring SMPCs for specific applications requiring large deformations and precise shape memory behavior. Future research should explore different fiber types, orientations, and programming conditions to further optimize the performance of SMPCs.

Acknowledgement: The authors express their gratitude to Indian Institute of Technology Madras for the support to carry out this work.

Funding Statement: The authors received no specific funding for this study.

Author Contributions: The authors confirm their contribution to the paper as follows: study conception and design: Kartikey Shahi; data collection: Boomurugan Ramachandran; analysis and interpretation of results: Kartikey Shahi, Velmurugan Ramachandran, Ranjith Mohan; draft manuscript preparation: Kartikey Shahi, Velmurugan Ramachandran, Ranjith Mohan. All authors reviewed the results and approved the final version of the manuscript.

Availability of Data and Materials: The data that support the findings of this study are available from the corresponding author upon reasonable request.

Ethics Approval: Not applicable.

Conflicts of Interest: The authors declare no conflicts of interest to report regarding the present study.

References

1. Liu T, Zhou T, Yao Y, Zhang F, Liu L, Liu Y, et al. Stimulus methods of multi-functional shape memory polymer nanocomposites: a review. Compos Part A: Appl Sci Manufact. 2017;100:20–30. doi:10.1016/j.compositesa.2017.04.022.
2. Lendlein A, Kelch S. Shape-memory polymers. Angew Chem Int Ed. 2002;41(12):2034–57.
3. Li T, Sun J, Leng J, Liu Y. An electrical heating shape memory polymer composite incorporated with conductive elastic fabric. J Compos Mat. 2022;56(11):1725–36. doi:10.1177/00219983221085630.
4. Yu K, Westbrook KK, Kao PH, Leng J, Qi HJ. Design considerations for shape memory polymer composites with magnetic particles. J Compos Mat. 2013;47(1):51–63. doi:10.1177/0021998312447647.
5. Liu C, Qin H, Mather PT. Review of progress in shape-memory polymers. J Mater Chem. 2007;17:1543–58.
6. Boudjellal A, Trache D, Khimeche K, Hafsaoui SL, Bougamra A, Tcharkhtchi A, et al. Stimulation and reinforcement of shape-memory polymers and their composites: a review. J Thermop Compos Mat. 2022;35(11):2227–60. doi:10.1177/0892705720930775.
7. Wei K, Zhu G, Tang Y, Li X, Liu T, Niu L. An investigation on shape memory behaviours of hydro-epoxy/glass fibre composites. Compos Part B: Eng. 2013;51:169–74. doi:10.1016/j.compositesb.2013.03.036.
8. Nishikawa M, Wakatsuki K, Takeda N. Thermomechanical experiment and analysis on shape recovery properties of shape memory polymer influenced by fiber reinforcement. J Mat Sci. 2010;45:3957–60. doi:10.1007/s10853-010-4545-x.
9. Meng Q, Hu J. A review of shape memory polymer composites and blends. Compos Part A: Appl Sci Manufact. 2009;40(11):1661–72. doi:10.1016/j.compositesa.2009.08.011.
10. Goda I, Zubair Z, L'Hostis G, Drean JY. Design and characterization of 3D multilayer woven reinforcements shape memory polymer composites. J Compos Mat. 2021;55(5):653–73. doi:10.1177/00219983209581.
11. Huang Y, Ren H, Liu Y, Xu W, Zhao W. Bending shape memory properties and multi-scale viscoelastic behaviors of knitted-fabric reinforced polymer composites. Compos Sci Technol. 2024;256(5):110747. doi:10.1016/j.compscitech.2024.110747.
12. Mu T, Liu L, Lan X, Liu Y, Leng J. Shape memory polymers for composites. Compos Sci Technol. 2018;160(1):169–98. doi:10.1016/j.compscitech.2018.03.018.
13. Xia Y, He Y, Zhang F, Liu Y, Leng J. A review of shape memory polymers and composites: mechanisms, materials, and applications. Adv Mater Weinheim. 2021;33(6):2000713. doi:10.1002/adma.202000713.
14. Rodriguez J, Giraldo D, Restrepo J, Colorado H. Cross-linked ethylene-vinyl acetate-poly(urethane) temperature-memory composite actuator. J Compo Mat. 2020;54(28):4441–55. doi:10.1177/0021998320933664.
15. Sun J, Liu Y, Leng J. Mechanical properties of shape memory polymer composites enhanced by elastic fibers and their application in variable stiffness morphing skins. J Intell Mat Syst Struct. 2015;26(15):2020–7. doi:10.1177/1045389X14546658.
16. Ahmad M, Luo J, Singh D, Miraftab M. Shape memory effect and thermomechanical properties of shape memory polymer fabric composite in tension mode. World J Eng. 2012;9(2):85–92. doi:10.1260/1708-5284.9.2.85.
17. Shakir Abbood I, aldeen Odaa S, Hasan KF, Jasim MA. Properties evaluation of fiber reinforced polymers and their constituent materials used in structures—a review. Mat Today: Proc. 2021;43:1003–8. doi:10.1016/j.matpr.2020.07.636.
18. Fu SY, Lauke B, Mäder E, Yue CY, Hu X. Tensile properties of short-glass-fiber- and short-carbon-fiber-reinforced polypropylene composites. Compos Part A: Appl Sci Manufact. 2000;31(10):1117–25. doi:10.1016/S1359-835X(00)00068-3.

19. Park SB, Lee JS, Kim JW. Effects of short glass fibers on the mechanical properties of glass fiber fabric/PVC composites. Mater Res Express. 2017 Mar;4(3):035301. doi:10.1088/2053-1591/aa6142.
20. Lin L, Zhou Q, Li M. Thermal and electroactive shape memory behaviors of polyvinyl alcohol/short carbon fiber composites. Poly Sci Series A. 2019;61:913–21. doi:10.1134/S0965545X1906004X.
21. Park M, Kim Y, Hwang JO, Park JK. Shape recovery characteristics of shape memory epoxy composites reinforced with chopped carbon fibers. Carbon Letters. 2019;29:219–24. doi:10.1007/s42823-019-00031-1.
22. Guo J, Wang Z, Tong L, Lv H, Liang W. Shape memory and thermo-mechanical properties of shape memory polymer/carbon fiber composites. Compos Part A: Appl Sci Manufact. 2015;76:162–71. doi:10.1016/j.compositesa.2015.05.026.
23. Ohki T, Ni QQ, Ohsako N, Iwamoto M. Mechanical and shape memory behavior of composites with shape memory polymer. Compos Part A: Appl Sci Manufact. 2004;35(9):1065–73. doi:10.1016/j.compositesa.2004.03.001.
24. Shahi K, Ramachandran V. Theoretical and experimental investigation of shape memory polymers programmed below glass transition temperature. Polymers. 2022;14(13):2753. doi:10.3390/polym14132753.
25. Li G, Wang A. Cold, warm, and hot programming of shape memory polymers. J Polym Sci Part B: Polym Phy. 2016;54(14):1319–39. doi:10.1002/polb.24041.
26. Yue L, Sun X, Yu L, Li M, Montgomery SM, Song Y, et al. Cold-programmed shape-morphing structures based on grayscale digital light processing 4D printing. Nat Commun. 2023;14(1):5519. doi:10.1038/s41467-023-41170-4.
27. Abishera R, Velmurugan R, Gopal KVN. Reversible plasticity shape memory effect in carbon nanotubes reinforced epoxy nanocomposites. Compos Sci Technol. 2016;137:148–58. doi:10.1016/j.compscitech.2016.10.030.
28. Abishera R, Velmurugan R, Nagendra Gopal KV. Reversible plasticity shape memory effect in carbon nanotube/epoxy nanocomposites: shape recovery studies for torsional and bending deformations. Polymer Eng Sci. 2018;58(S1):E189–98. doi:10.1002/pen.24861.
29. Shahi K, Boomurugan R, Velmurugan R. Cold programming of epoxy-based shape memory polymer. Structures. 2021;29:2082–93. doi:10.1016/j.istruc.2020.05.023.
30. Xie T, Rousseau IA. Facile tailoring of thermal transition temperatures of epoxy shape memory polymers. Polymer. 2009;50(8):1852–6. doi:10.1016/j.polymer.2009.02.035.
31. Sato N, Kurauchi T, Sato S, Kamigaito O. Mechanism of fracture of short glass fibre-reinforced polyamide thermoplastic. J Mat Sci. 1984;19:1145–52. doi:10.1007/BF01120023.
32. Sato N, Kurauchi T, Sato S, Kamigaito O. Microfailure behaviour of randomly dispersed short fibre reinforced thermoplastic composites obtained by direct SEM observation. J Mat Sci. 1991;26:3891–8. doi:10.1007/BF01184987.
33. Simonini L, Mahmood H, Dorigato A, Pegoretti A. Tailoring the physical properties of poly(lactic acid) through the addition of thermoplastic polyurethane and functionalized short carbon fibers. Polymer Compos. 2023;44(8):4719–33. doi:10.1002/pc.27435.
34. Nguyen TD, Jerry Qi H, Castro F, Long KN. A thermoviscoelastic model for amorphous shape memory polymers: incorporating structural and stress relaxation. J Mech Phys Solids. 2008;56(9):2792–814. doi:10.1016/j.jmps.2008.04.007.
35. Takahashi K, Choi NS. Influence of fibre weight fraction on failure mechanisms of poly(ethylene terephthalate) reinforced by short-glass-fibres. J Mater Sci. 1991;26(17):4648–56. doi:10.1007/BF00612401.
36. Simonini L, Mahmood H, Dorigato A, Pegoretti A. Evaluation of self-healing capability of a polycaprolactone interphase in epoxy/glass composites. Compos Part A: Appl Sci Manufact. 2023;169:107539. doi:10.1016/j.compositesa.2023.107539.
37. Aharoni SM. Increased glass transition temperature in motionally constrained semicrystalline polymers. Polym Adv Technol. 1998;9(3):169–201. doi:10.1002/(SICI)1099-1581(199803)9:3<169::AID-PAT740>3.0.CO;2-Z.
38. Do NBD, Imenes K, Aasmundtveit KE, Nguyen HV, Andreassen E. Thermal conductivity and mechanical properties of polymer composites with hexagonal boron nitride—a comparison of three processing methods: injection moulding, powder bed fusion and casting. Polymers. 2023;15(6):1552. doi:10.3390/polym15061552.